coatings

MDPI

Article

Fluorescent Silica Hybrid Film-Forming Materials Based on Salicylaldazine

Alina Raditoiu [1], Valentin Raditoiu [1,*], Florentina Monica Raduly [1], Georgiana Cornelia Ispas [1], Violeta Purcar [1], Adriana Nicoleta Frone [1], Raluca Manea [1], Luminita Eugenia Wagner [1] and Mihai Anastasescu [2]

[1] Laboratory of Functional Dyes and Related Materials, National Research and Development Institute for Chemistry and Petrochemistry—ICECHIM, 202 Splaiul Independentei, 6th District, 060021 Bucharest, Romania; coloranti@icechim.ro (A.R.); monica.raduly@icechim.ro (F.M.R.); georgiana.ispas@icechim.ro (G.C.I.); violeta.purcar@icechim.ro (V.P.); adriana.frone@icechim.ro (A.N.F.); raluca.manea@icechim.ro (R.M.); luminitawagner@yahoo.com (L.E.W.)

[2] Surface Chemistry and Catalysis Laboratory, Institute of Physical Chemistry "Ilie Murgulescu" of the Romanian Academy, 202 Splaiul Independentei, 060021 Bucharest, Romania; manastasescu@icf.ro

* Correspondence: vraditoiu@icechim.ro

Received: 28 November 2020; Accepted: 16 December 2020; Published: 18 December 2020

Abstract: Fluorescent film-forming materials were obtained by embedding salicylaldazine (SAA) in silica hybrids generated by sol–gel processes from different silane precursors in acid catalysis. Tuned local environments for the fluorophore were generated in the hosting network by modifying silica sols with organic groups through the co-condensation of tetraethylortosilicate (TEOS) and different alkoxysilanes hydrolysis products. The photophysical properties of the luminescent hybrid films were studied in direct relationship with structural, textural, and surface properties and based on interactions between SAA species and the silica hosting network. Film-forming materials were studied in order to determine differences in absorption and fluorescence emission due to the environments around the fluorophore. The variations recorded in the fluorescence emission spectra of the hybrid films were related to interactions established between the fluorophore species and their sterically hindered surroundings of the host hybrid silica, where free molecular motions are restricted. The influence of the type and amount of network modifier and of the fluorophore loading on the transparency of the films and fluorescence intensity was also investigated. The study carried out led to the elucidation of the necessary conditions for obtaining luminescent film-forming materials with high luminescence intensity and transparency useful for the design of new light concentrators.

Keywords: fluorescence emission; hybrid films; sol-gel; cyclic oligomers; porosity

1. Introduction

Salicylaldazine and several analogs were intensively studied due to their fluorescent properties [1–3]. This type of fluorophores owes their special optical properties, such as strong solid state luminescence and tunable emission, to the environment-sensitive excited state based on intramolecular proton transfer (ESIPT) mechanism, which is responsible for the luminescence. Restricted molecular motions in the excited state and the absence of the radiative deactivation pathways lead to an enhancement of luminescence in solid state comparatively with solutions showing a large Stokes shift. Dyes exhibiting this type of luminescence mechanism can be used as sensors, fluorescent tracers in biology, in electroluminescent devices, laser dyes [3], etc. Since ESIPT emission is highly sensitive to local surroundings and the presence of hydrogen bond-donating species can lead to inhibition of the process, this type of fluorophores is widely used for the detection of chemical or biological targets [4].

In recent years, hybrid silica materials became the most used host matrices for organic dyes entrapped or covalently linked [5] into the network, as a result of imparting outstanding optical, mechanical, and thermal properties to the host–guest composite systems. Moreover, modification of the type and amount of organic groups in the hybrid silica materials determined a fine tuning of the dye molecules' environmental surroundings [6]. Therefore, this type of composite materials gained importance for optical devices, such as light concentrators, optical waveguides, or laser dyes [7].

Several studies on fluorescent dyes show that fluorescence intensity can be influenced after incorporation into a certain type of hosting matrices due to intermolecular energy transfer processes. By varying the environmental surroundings, the dye molecules absorption and fluorescence emission maxima are shifted due to intermolecular interactions established with inorganic silanol groups or with organic groups grafted at the surface of silica matrices [8]. Moreover, in order to enhance the emission efficiency and to gain temporal stability of the luminescence, SAA or other luminophores of this type should be embedded in rigid matrices as a general requirement for technical applications [9].

The idea of using molecular systems exhibiting ESIPT characteristics to solar concentrators is relatively new [10,11] and is based on an increased flexibility through tailoring intermolecular interactions. However, tuning molecular aggregation in solid state by using hybrid sol–gel generated film-forming materials can be an effective way to achieve the tunable emission of such materials, and SAA can serve as a molecular model in this sense [12]. Nevertheless, among other types of fluorophore dyes, SAA display aggregation-induced emission enhancement (AIEE), which can be seen when the SAA content was increased. This is the explanation for the high solid-state fluorescence intensity recorded for SAA by comparison with the most organic fluorophores, which show fluorescence quenching in solid state [13].

In particular, some drawbacks of other types of fluorophores are related to poor environmental stability and light-fastness, often small Stokes shifts and therefore high reabsorption, limited quantum efficiency, and high toxicity due to the heavy metals in their structure [13].

Therefore, the objective of our work was to investigate the photoluminescent properties of some materials containing SAA entrapped in silica hybrid matrices, as attractive optical film-forming systems, previously investigated by us as antireflective coatings [14], which can be obtained by using a facile preparation method. Based on the special intrinsic properties of phenol-keto equilibrium [15,16] combined with the effect of interactions between the embedded fluorophore and the host matrices, the study can lead to important findings about the possibilities of tuning the optical properties of this type of luminescent films, in order to obtain highly luminescent and transparent hybrid silica films, having large Stokes shifted fluorescence emission, which is useful for the design of new luminescent solar concentrators (LSC) especially designed for integrated solar windows.

2. Materials and Methods

2.1. Materials

Hydrochloric acid (0.1 N, HCl, Chimreactiv, Bucharest, Romania) and 1-methylimidazole (98%, NMI, Merck, Kenilworth, NJ, USA) were used as catalysts. Tetraethylortosilicate (98%, TEOS, Aldrich, St. Louis, MO, USA), phenyltriethoxysilane (97%, PTES, Aldrich, St. Louis, MO, USA), diphenyldiethoxysilane (98%, DPDES, Aldrich, St. Louis, MO, USA), 3-glycidoxypropyltriethoxysilane, (98%, GPTES, Aldrich, St. Louis, MO, USA), octyltriethoxysilane (97%, OTES, Aldrich, St. Louis, MO, USA), dimethyldiethoxysilane (98%, DMDES, Aldrich, St. Louis, MO, USA), methyltriethoxysilane (99%, MTES, Aldrich, St. Louis, MO, USA) were used, first as a network generator and the others were used as network-modifier agents. Ethanol (96%, EtOH, Chimreactiv, Bucharest, Romania), tetrahydrofuran (99%, THF, Merck, Kenilworth, NJ, USA), N,N-dimethylformamide (98%, DMF, Merck, Kenilworth, NJ, USA) and hexane (99%, Hx, Merck, Kenilworth, NJ, USA) were used as solvents. Hydrazine hydrate (80%, HZ, Merck, Kenilworth, NJ, USA) and salicylaldehyde (98%, SA, Merck,

Kenilworth, NJ, USA) were used as reactants for the synthesis of SAA. All the chemicals were used as received without further purification.

2.2. Synthesis Methods

2.2.1. SAA Synthesis

The fluorophore is obtained using a method already presented in the literature [9]. Briefly, a mixture of SA (10.38 g, 83 mmol) and HZ (1.6 mL, 42 mmol) in 100 mL EtOH was refluxed for 6 h. On cooling, pale-yellow solid precipitated was filtered and recrystallized from methanol.

2.2.2. Fluorescent Film-Forming Materials

In order to obtain fluorescent film-forming materials, mixtures of 1.6 mL of TEOS and 1.6 mL of a network modifying agent (PTES, MTES, OTES, DPDES, DMDES, and GTES), 2 mL of THF containing 0.022 g SAA, 2.2 mL of EtOH, and 0.75 g of HCl were stirred for 3 h at room temperature. Fluorescent powders were obtained after grounding in a ceramic mortar, and solid materials resulted after the evaporation of residual solvents and water from film-forming solutions placed into plastic vials. Films and powders were denoted as a function of the network modifying agent: G1(PTES); G2(MTES), G3(OTES), G4(DPDES), G5(DMDES), G6(GTES), and G0 for the material obtained without the addition of a modifying agent. The solutions were deposited by dip-coating on microscope glass slides previously cleaned in hydrogen peroxide solution (30%) and acetone. Films were dried at room temperature for 24 h and subsequently heated to 100 °C for 1 h in a vacuum oven.

2.3. Characterization Methods

Fourier Transform Infrared (FTIR) spectra of hybrid materials were obtained on a JASCO FT-IR 6300 instrument (Jasco Int. Co. Ltd., Tokyo, Japan), equipped with a Specac ATR Golden Gate (Specac Ltd., Orpington, UK) with KRS5 lens, in the range 400–4000 cm^{-1} (32 accumulations at a resolution of 4 cm^{-1}) and processed with Spectra Manager II software (Jasco Int. Co. Ltd., Tokyo, Japan).

Diffuse reflectance and transmission spectra were recorded in the range 380–780 nm on a JASCO V570 UV-VIS-NIR spectrophotometer (Jasco Int. Co. Ltd., Tokyo, Japan), equipped with a JASCO ILN-472 (150 mm) integrating sphere, using spectralon as reference. They were processed with Spectra Manager I software (Jasco Int. Co. Ltd., Tokyo, Japan).

Fluorescence spectra were recorded with a JASCO FP 6500 spectrofluorimeter (Jasco Int. Co. Ltd., Tokyo, Japan), at 25 °C, using 10 mm path-length quartz cuvettes for liquids or the device for solid samples at an excitation wavelength of 365 nm and processed with Spectra Manager I software (Jasco Int. Co. Ltd., Tokyo, Japan). Fluorescence absolute quantum yields were measured using a Jasco ILF 835 integrating sphere unit attached to the spectrofluorimeter.

Atomic Force Microscopy (AFM) measurements were performed using an XE-100 instrument (Park Systems, Suwon, Korea), equipped with flexure-guided and cross talk eliminated scanners. Images were recorded in non-contact mode, with sharp tips of NCHR type (Nanosensors TM, Neuchatel, Switzerland) and were processed with XEI software v.1.8.0 (Park Systems, Suwon, Korea).

Contact angle measurements were obtained using a CAM 200 optical contact angle and surface tension goniometer (KSV Instruments, Helsinki, Finland) equipped with a high-resolution camera Basler A602f (Basler AG, Ahrensburg, Germany) and an auto dispenser. A small droplet of deionized water was placed onto the surface of each sample using a micro-syringe in order to measure the static contact angle by analyzing the shape. The values of the static water contact angle were obtained as the average of ten measurements in various zones of the samples.

Nitrogen sorption isotherms were recorded on a Quantachrome Nova 2200e automated gas adsorption system (Quantachrome Instruments, Boynton Beach, FL, USA) at the liquid nitrogen temperature (−196 °C). All of the samples were outgassed at 150 °C for 3 h under vacuum prior to

nitrogen adsorption. The pore volume and area distributions were calculated using Barrett, Joyner, and Halenda (BJH) method.

3. Results and Discussion

3.1. Photophysical Properties of SAA in Solution

The study of the SAA behavior in solution revealed that the absorption maxima are very little influenced by the polarity of the solvents. UV-Vis absorption spectra showed the presence of a single broad band centered at 360 nm, corresponding to the phenolic tautomer, as it can be seen in Table 1.

Table 1. Photophysical characteristics of salicylaldazine (SAA) (10^{-4} M) in different solvents.

Solvent (Polarity Index)	DMF (6.4)	EtOH (5.2)	THF (4.0)	Hx (0.0)
Absorption wavelength (λ_{abs}, nm)/Optical density (a.u.)	357/2.2	357/2.3	359/2.02	360/2.2
Fluorescence wavelengths ($\lambda_{1f}/\lambda_{2fl}$, nm)/Intensity (a.u.)	547/418 201/88	547/418 14/3	547/418 252/98	547/418 22/7
Stokes shift (SS, nm)	190	190	188	187

Increasing the polarity of the solvent did not significantly influence the position of the absorption band, while any phenol-keto equilibrium in solution, in the ground state, cannot be detected. This is due to the phenolic form stabilization through an intramolecular hydrogen bond established between the hydrogen atom of the phenolic group and the relatively highly basic nitrogen atom of the azine group. This property makes the difference between SAA and other Schiff bases in which the nitrogen atom basicity is diminished as a result of the conjugation with the aromatic rest bond to it. Additionally, SAA stability to hydrolysis among other Schiff bases can be also explained by this particularity of the hydrogen bond. In this context, SAA is an appropriate fluorophore to be embedded in silica hybrid sol-gel generated materials, in which the presence of water and protic catalysis hypothetically could lead to SAA hydrolysis.

The analysis of fluorescence emission in solution showed that SAA exhibit two emission bands situated at 418 and 547 nm, irrespective of the solvent polarity. The short-wavelength emission corresponding to the phenolic tautomer is very weak in nonpolar or protic solvents, while in aprotic dipolar solvents, the intensity of the emission become more than ten times higher. The most important emission band originating from the cis-keto tautomer is situated at a longer wavelength and has an intensity up to five times higher than the previous.

The Stokes shift values are large in all cases and confirm minimization of the possibility for emission reabsorption.

3.2. Photophysical Properties of Fluorescent Hybrid Materials

After embedding SAA in silica-based materials, some important changes in the fluorescence spectra were observed. The silanol free groups at the surface of hybrid materials will determine the stabilization of the fluorophore molecules and will influence the fluorescence spectra of the hybrids, as it was previously shown for protic solvents. Moreover, during the preparation of sol-gel silica materials, pores of the silica network are filled with water, EtOH, and THF, which formed the nearest environment of SAA molecules. After drying, the SAA nearest environment is formed of organic groups from network modifier and silanol residues from TEOS hydrolysis. Therefore, the network modifying agents used in the synthesis of film-forming materials modulate the interactions between the fluorescent dye and the host matrix.

Luminescence enhancement in the solid state is characteristic for molecules presenting fluorescence based on the ESIPT mechanism. Therefore, after gelation and drying of the silica hybrid films,

the fluorescence emission is due to intramolecular hydrogen bonds and associations between dye molecules or with network silica neighboring groups.

In the case of G0 fluorescent film, the interaction of SAA with silanol groups (Si–OH) by intermolecular hydrogen bonds leads to a batochromic of the short-wavelength emission band, while the "cis-keto" band is blue shifted. The latter is red shifted with about 9–12 nm in the case of hybrid materials modified with large organic groups (G1, G3, and G4). An explanation can be the formation of significant larger pores in the structure of the network because of the size of organic modifiers. In these pores, there can be found aggregated SAA molecules, favoring the stabilization of cis-keto species by intramolecular hydrogen bonds because interactions of SAA with silanol groups are prevented. This is confirmed by the higher intensity of the fluorescence emission and fluorescence efficiency, as can be observed from Table 2, which is an important finding characterizing ESIPT molecules, as it was also observed by other authors [17,18]. However, when aromatic groups are present as organic modifiers in the structure of the network (G1, G4), π–π interactions with SAA molecules also take place, diminishing fluorescence intensity, by comparison with G0. Therefore, in this case, the quenching or shifting of the fluorescence emission peak is due to the interactions established between dye species and silica network modifier.

Table 2. Photophysical characteristics of SAA (1% by weight) embedded in hybrid films.

Sample	G0	G1	G2	G3	G4	G5	G6
Absorption wavelength (λ_{abs}, nm)	347	362	358	359	364	363	347
Fluorescence wavelength (λ_{fl1}, nm)/(Intensity, a.u.)	440 (20)	438 (7)	439 (13)	438 (8)	434 (17)	437 (7)	434 (56)
Fluorescence wavelength (λ_{fl2}, nm)/(Intensity, a.u.)	534 (217)	543 (185)	536 (219)	546 (93)	545 (155)	536 (243)	533 (89)
Stokes shift (SS, nm)	187	181	198	187	181	173	186
Sample absorbance (%)	82.7	88.9	90.2	81.1	85.4	83.5	89.7
External quantum efficiency (%)	0.01	3.06	2.13	3.38	1.73	2.69	1.64
Internal quantum efficiency (%)	0.02	3.46	2.37	4.18	2.03	3.44	1.83

The Stokes shift has the smallest value in the case of G5, because two methyl groups in the molecule of network modifier provide sufficient steric hindrance to limit SAA interaction with silanol groups, on the one side, and on the other side, they do not interact in any way with the fluorophore. On the contrary, the Stokes shift recorded for G2 has the highest value in the series because of the minimum steric hindrance provided by the existence of only one methyl group in the molecule of the network modifier, which is not able to prevent entirely interactions of SAA with silanol groups.

A special situation was found for G6 films, in which the generation of hydroxyl groups during epoxy groups' homopolymerization leads to a stabilization of the enol tautomer through intermolecular hydrogen bonds. As a result, the short wavelength emission intensity increased significantly.

As a preliminary finding, the highest intensity of the emission peak was recorded for G5, while the quantum yield is among the highest in the series. It is obvious that intramolecular interactions and the aggregation of SAA in constrained environments will determine the photophysical properties of this type of hybrid films and fluorescence emission parameters recommend them to be further investigated in more detail.

3.3. Structural Characterization by ATR FTIR Spectroscopy

Structural characteristics of silica hybrids are the main factors that decisively determine the behavior of fluorescent films and their photophysical properties.

Silica material G0 generated from TEOS showed a broad absorption band at 3271 cm^{-1}, which is due to the stretching vibration of hydroxyl groups involved in hydrogen bonds. The bending vibration of water molecules is at around 1623 cm^{-1}, while at 933 cm^{-1} can also be seen a broad band corresponding to the stretching vibration of Si–OH groups. All these bands are correlated with the formation of hydroxyl groups during TEOS hydrolysis and present displacements or modifications

when network-modifying agents are added to TEOS in order to generate hybrid silica networks by sol–gel hydrolysis–condensation. As a remark, in this case, the absorption band due to Si–O–Si stretching vibration is located at 1055 cm^{-1}.

Analysis of the FTIR spectra showed characteristic bands for each type of organic network modifier. Therefore, in the case of alkyl groups, the asymmetric and the symmetric stretching vibrations of the methylene group are found at 2924–2927 and 2855–2870 cm^{-1}, respectively. The stretching vibration of the CH aromatic groups is seen around 3050–3070 cm^{-1}, while for methyl groups, it is found at 2965 cm^{-1}. The broad band characteristic for hydrogen-bonded O-H groups is situated at 3271–3372 cm^{-1} and is shifted to higher wavenumbers as the capacity of the organic group belonging to the modifier to hinder the formation of hydrogen bonds is higher. Moreover, in the case of G1, G3, and G4 are seen bands corresponding to the stretching vibration of free O–H groups situated at 3598–3685 cm^{-1}.

Characteristic bands for the organic groups grafted onto the silica network are also found, as it can be seen in Figure 1. Thus, a sharp band attributed to $\delta(H_3C–Si)$ symmetric deformation was observed at 1270 cm^{-1} and another band was found at 771 cm^{-1} corresponding to $\gamma(H_3C–Si)$ in the case of G2. The first one is shifted to 1260 cm^{-1} and the second is split into two bands at 844 and 796 cm^{-1} in the case of G5. For aromatic rings, two sharp bands at 1595 and 1431 cm^{-1} are characteristic, and in the pattern zone, there are two bands at 736 and 694 cm^{-1} for G1, while for G4, the sharp bands are displaced at 1592 and 1429 cm^{-1} and in the pattern zone, three bands situated at 739, 716 and 695 cm^{-1} are identified, respectively.

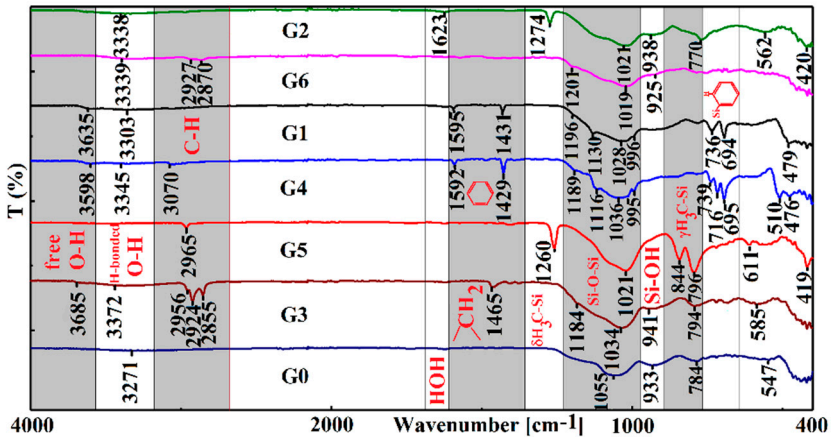

Figure 1. Attenuated Total Reflectance (ATR)-Fourier Transform Infrared (FTIR) spectra of fluorescent silica hybrids.

In the zone of Si–O–Si and Si–OH stretching vibrations, bands are visibly affected by the presence of organic groups grafted onto the silica network. The presence of cyclic and linear Si–O–Si fragments determine some peaks at about 1088 and 1050 cm^{-1}, respectively. The ratio between their intensities reflects changes in the formation of cyclic and linear structures during the sol–gel process, as it will be further shown.

3.4. Properties of Fluorescent Dimethyl-Modified Silica Films

3.4.1. Influence of the Amount of DMDES

During the hydrolysis–condensation of TEOS, catalyzed by acids, a lot of residual hydroxyl groups are generated on the surface of the silica materials. When network-modifying agents are used in the sol-gel process together with TEOS, organic groups from the modifier interfere with the residual hydroxyl groups. When trialkoxysilane derivatives are used as network modifiers, randomly distributed organic groups are usually formed, while dialkoxysilane derivatives can lead to linear

chains intercalated in the silica network. Thus, hydrophobic domains can be formed preferentially inside the network. In this case, the transmittance of the film can suffer because of the material inhomogeneity and differences of refractive indices, which can lead to a translucent material.

Several studies showed that during hydrolysis–condensation, the amount of linear oligomeric structures increased in the beginning, while at the end, cyclization became dominant on the account of the latter [19], which is a process that can be followed by FTIR spectroscopy [20]. Another finding is that the ratio of cyclic to linear form decreases as the amount of DMDES decreases, as already observed from NMR studies [21,22]. Analysis of FTIR spectra shows that a small amount of DMDES decreases the gelation time and higher amounts decrease the functionality and lead to an increasing of the content of cyclic species. At lower DMDES loadings, the gelation time is reduced because the hydrolysis reaction rate is higher than that of TEOS. When the amount of DMDES increases, cyclic oligomers decrease the average functionality, and the gelation time increases. Therefore, the stretching vibration of the Si–O–Si group of the linear form is shifted from 1055 cm^{-1}, in the case of G0 to 1019 cm^{-1} for G5, when the weight ratio is TEOS:DMDES = 1:1 ($G5_{50}$). Simultaneously, a shoulder is formed at 1085 cm^{-1}, when the weight ratio is TEOS:DMDES = 3:1 ($G5_{25}$), corresponding to the stretching vibration of the Si–O–Si group of the cyclic form. The intensity of the shoulder corresponding to the cyclic form increased, and the band is shifted to 1061 cm^{-1} in the case of $G5_{50}$.

Another characteristic of the FTIR spectra is the decreasing of the band at 939 cm^{-1}, which is due to the decrease of the amount of Si–OH groups formed during TEOS hydrolysis. The hydrophobic character of the films increased as the amount of DMDES increased, which can be observed from the shifting of OH stretching vibration from 3272 cm^{-1} for G0 to 3476 cm^{-1} for $G5_{50}$, as it can be seen from Figure 2.

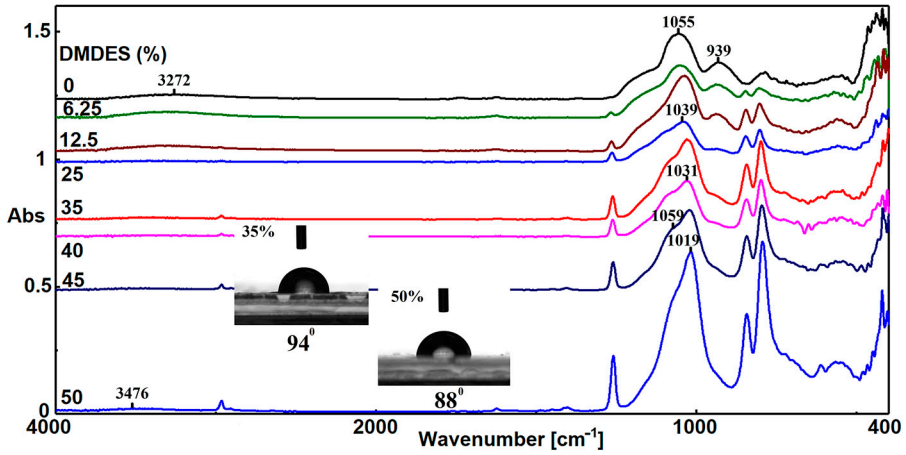

Figure 2. ATR-FTIR spectra and water contact angle of some G5 films obtained at different dimethyldiethoxysilane (DMDES) loadings.

The measurement of the water contact angle sustains that hydrophobic domains are formed inside the network, as the amount of DMDES is increased, due to the formation of cyclic structures. Thus, the mean contact angle of water on the surface of the $G5_{25}$ film is 94° ± 1°, which is greater than that of the $G5_{50}$ film, which is 88° ± 2°. This behavior is determined by the facile migration of cyclic oligomeric structures to the film surface during the gelation of $G5_{25}$, as it will be shown below.

Surface morphology of the fluorescent films was investigated by atomic force microscopy (AFM) in order to elucidate the influence of DMDES loadings on topographical and textural changes. Consequently, the analysis showed if the morphology influences whether the films' surface becomes hydrophilic or hydrophobic. Measurements made on a surface area of 1 × 1 μm^2, during analysis of two-dimensional AFM images, showed minor textural changes between $G5_{25}$ and $G5_{50}$ hybrid films, as it can be seen in Figure 3.

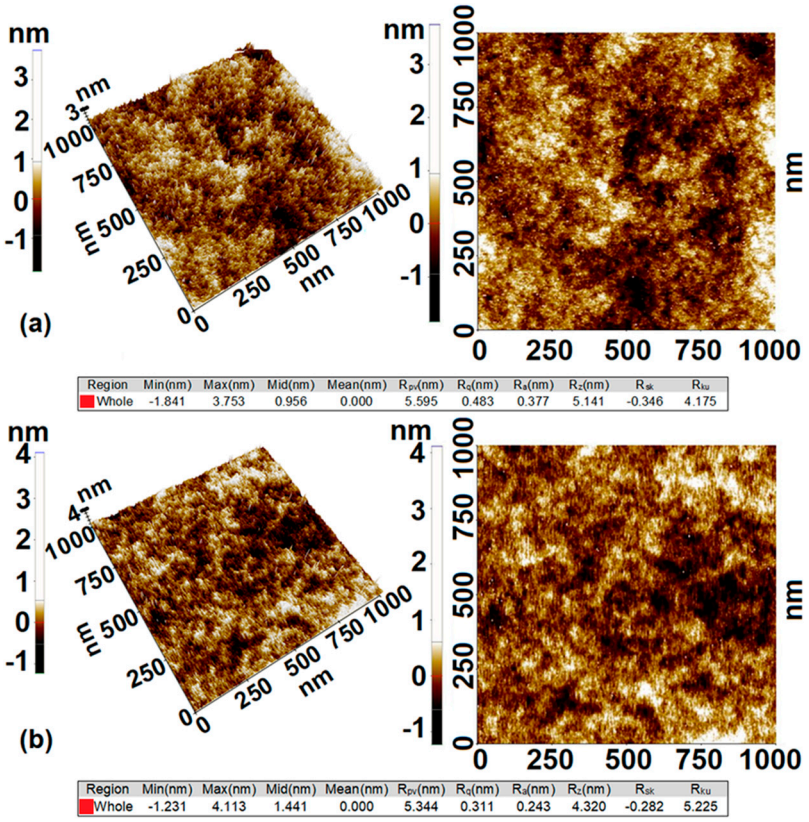

Figure 3. AFM images of G5 hybrid films at 25% (**a**) and 50% (**b**) DMDES loadings.

Both samples are very smooth with root mean square roughness (R_q) around 0.48 nm for $G5_{25}$ and 0.31 nm for $G5_{50}$. This parameter may be one of the factors that influence the overall results obtained for the mean water contact angle. However, several studies showed that small variations in the nanometer surface roughness may contribute to the hydrophobic behavior of surfaces similarly to that caused by the micron texture [23].

The surface roughening at medium DMDES loadings ($G5_{25}$) is due to the nanometer-sized surface migration of cyclic oligomers, while for $G5_{50}$ films, the higher viscosity of the sols during gelation, in spite the formation of a larger amount of cyclic species, prevent a massive migration of them to the surface. Thus, the wetting properties of the $G5_{50}$ surface are influenced especially by the residual silanol groups generated during TEOS hydrolysis and corresponding methyl groups from co-condensation with DMDES. The co-condensation is sustained by other studies [24,25], which demonstrate that hydrolyzed TEOS is more likely to co-condensate with DMDES than to self-condensate or to further hydrolysate.

In order to complete the picture of the films' topography, the difference between the deepest and the highest points in the scanned surface is given by the peak-to-valley parameter (R_{PV}), which is estimated to be 5.6 and 5.34 nm for $G5_{25}$ and $G5_{50}$, respectively. Therefore, it can be stated that the higher the amount of DMDES, the smoother the surface of the hybrid films. It should be mentioned that samples having an amount of DMDES higher than 50% by weight were not studied because they showed a phase separation during sol–gel processes and are translucent, as already observed by other authors [26,27].

The analysis of the films porosity shows some interesting results. Therefore, increasing the amount of DMDES up to 25% by weight, the pore volume reduces, while over this limit, the pore volume increases, as it can be seen in Table 3. The filling effect due to SAA molecules and the retardance of the network crosslinking process seem to be two main reasons for the reducing of the pore volumes. However, when the amount of DMDES increases, the less condensed character leads to the increase of

the micropores volume especially due to the self-condensation of DMDES and formation of oligomeric structures, as intercalated into the silica network.

Table 3. Textural properties of G5 hybrid films at different DMDES loadings.

DMDES (%)	S_{BJH} ($m^2 \cdot g^{-1}$)	$V_{BJH} \times 10^3$ ($cm^3 \cdot g^{-1}$)	D_{pore} (nm)	µpore S ($m^2 \cdot g^{-1}$)	µpore $V \times 10^3$ ($cm^3 \cdot g^{-1}$)
0	1.72	2.5	3.3	3.05	1.1
12.5	2.05	2.8	3.3	2.66	0.9
25	1.79	2.2	3.1	6.54	2.1
50	3.55	4.8	3.3	8	2.8

Regardless of DMDES loading, hybrid materials have a narrow pore size distribution with an average pore size of 3.3 nm. At low DMDES loadings, the filling effect leads to a small and narrow micropore size distribution and reduction of pore volume, the mesoporosity is more pronounced, and the number of micropores is lower, while when the DMDES loading increases up to 50%, the microporosity becomes important and determines the formation of a less condensed material with increased pore volume.

The decrease of the pore size, up to the SAA molecules, at low DMDES loadings determined the stabilization of the SAA enol form, with consequences on the fluorescence emission and absorption spectra. The existence of no interaction between methyl groups from the hybrid silica and SAA molecules leads to the formation of self-associated SAA molecules, explaining the yellowing effect which is more pronounced at low loadings of DMDES, as it can be observed from Figure 4a.

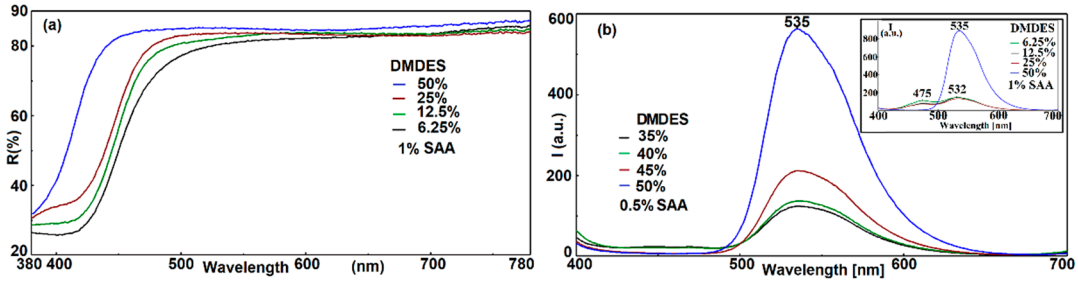

Figure 4. Reflectance (**a**) and fluorescence emission spectra (**b**) of G5 films at different DMDES loadings. (The inset shows the intensity of fluorescence emission at lower DMDES loadings).

The close microenvironment determines the appearance of a single intense or a dual emission band due to the keto tautomer in the excited state, as can be seen from Figure 4b or to the presence of both tautomers, enol and keto with emission bands centered at 475 and 532 nm, respectively, as in the inset of Figure 4b. The latter situation is encountered at moderate and low DMDES loadings as a result of decreasing the micropores' volume.

3.4.2. Influence of the Amount of SAA

ESIPT molecules such as SAA show several characteristics that make them valuable candidates for obtaining fluorescent devices. As it was already reported [28], SAA and its derivatives did not obey empirical rules on solid-state fluorescence due the intramolecular hydrogen bond, which is essential for fluorescence and because this molecular property is retained in the solid state. Therefore, the limit of the amount of SAA in hybrid silica films is determined by other factors than the fluorescence quenching, because increasing the SAA amount leads to a higher fluorescence intensity.

One of the factors is the transmittance of the hybrid film, because fluorescent films in light concentrators must have a high value of transmittance. In the case of G5 hybrid films, higher SAA loadings increases the fluorescence intensity, but the transparency decreases as a result of light scattering.

This is due to aggregation of SAA molecules by hydrogen bonding and π–π stacking interactions and the segregation of aggregates in the hybrid film. In the case of $G5_{50}$ hybrid films, the upper limit is 1% SAA by weight, which leads to a transmittance value higher than 92%, as can be seen in Figure 5a. Beyond this limit, the films become much less transparent. The transmittance of the same film containing 2% by weight SAA decreases significantly below 90%, which is unacceptable for the envisaged application.

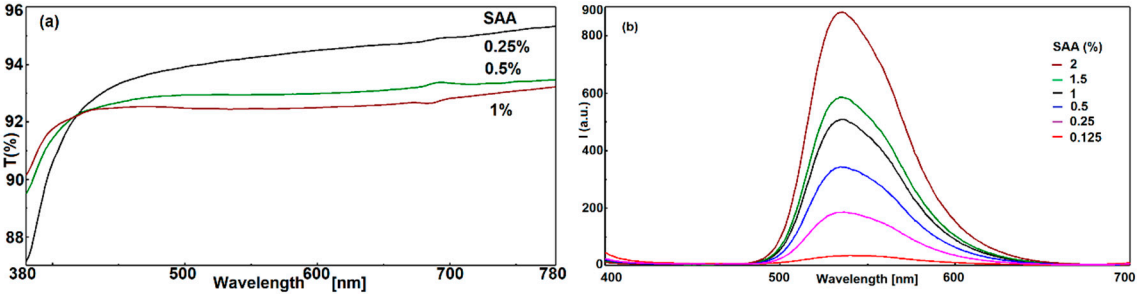

Figure 5. The transmittance (**a**) and fluorescence spectra (**b**) of G5 hybrid films containing different amounts of SAA.

In order to investigate the influence of SAA loading on the fluorescence emission spectra of G5 hybrid films, several materials containing different quantities of fluorophore were studied, as it is showed in Figure 5b. As it was previously demonstrated, by increasing the fluorophore concentration, a more pronounced association of SAA molecules takes place, and simultaneously, the intensity of fluorescence emission increases. The fluorescence emission wavelength is not affected, because interactions are established only between SAA molecules and is very little affected by the silica network, when DMDES is used in high quantities as network modifier. However, the quantity of fluorophore in the hybrid films cannot be larger than 1% by weight, because aggregation and segregation phenomena including fluorophore crystallization take place, affecting optical properties, especially the transmittance of the films.

4. Conclusions

Fluorescent film-forming materials were prepared by embedding salicylaldazine in silica hybrids generated by sol-gel processes from different silane precursors in acid catalysis, and their photophysical properties were investigated.

The interaction between the fluorophore and the host matrix and the pathways to influence these interactions by appropriately modifying the host matrix structure were studied. The formation of small rings during the sol–gel process by a kinetically favored reaction over chain extension and the migration of oligomeric structures to the surface of the films have an important influence on the photophysical properties of the luminescent materials.

Among the structure, the hydrophobicity and porosity of the hybrid materials are controlled by the amount of silica network modifier and determine the photophysical behavior of the salicylaldazine dye. DMDES was proved to provide optimal conditions for maximum fluorescence emission intensity and high transparency of the films, over 92% in the visible range, when the salicylaldazine content is up to 1% by weight. The stabilization of the emission band originating from the cis-keto tautomer provides a large Stokes shift of more than 150 nm, reducing the possibility of self-absorption and producing suitable film-forming materials for studying the design of new light concentrators.

However, some limitations still remain unsolved, as can be observed from the study, namely the limitation of the amount of SAA in the film-forming materials, because at high SAA loadings, the transmittance of the films decreased under the limit of 90%, which is unacceptable for such applications. Other drawbacks are the quantum efficiency, which is still lower, 4–5%, and the maximum

amount of network modifier (DMDES) in the silica film-forming materials, which cannot exceed 50% by weight, because the crosslinking of the hybrid network is negatively influenced and affects the stability and physical–chemical properties of the coatings.

Author Contributions: Conceptualization, V.R.; methodology V.R. and A.R.; formal analysis, A.R., G.C.I., F.M.R., and M.A.; investigation, V.P. and R.M.; resources, M.A., V.R., and A.N.F.; data curation, A.R. and A.N.F.; writing—original draft preparation, V.R.; writing—review and editing, V.R. and G.C.I.; supervision, L.E.W.; project administration, A.R. All authors have read and agreed to the published version of the manuscript.

Funding: This research was funded by Romanian Ministry of Education and Research—MEC through INCDCP ICECHIM Bucharest 2019–2022 Core Program PN. 19.23—Chem-Ergent, grant number 19.23.03.04. The APC was funded by INCDCP ICECHIM Bucharest.

Conflicts of Interest: The authors declare no conflict of interest. The funders had no role in the design of the study; in the collection, analyses, or interpretation of data; in the writing of the manuscript, or in the decision to publish the results.

References

1. Ammar, A.H.; El-Sayed, B.A.; El-Sayad, E.A. Structural and optical studies on ortho-hydroxy acetophenone azine thin films. *J. Mater. Sci.* **2002**, *37*, 3255–3260. [CrossRef]
2. Satam, M.A.; Telore, R.D.; Sekar, N. Pigment Yellow 101 analogs from 3-(1,3-benzothiazol-2-yl)-2-hydroxynaphthalene-1-carbaldehyde—synthesis and characterization. *Dyes Pigments* **2015**, *123*, 274–284. [CrossRef]
3. Satam, M.A.; Telore, R.D.; Sekar, N. Photophysical properties of Schiff's bases from 3-(1,3-benzothiazol-2-yl)-2-hydroxy naphthalene-1-carbaldehyde. *Spectrochim. Acta Part A Mol. Biomol. Spectrosc.* **2014**, *132*, 678–686. [CrossRef]
4. Sedgwick, A.C.; Wu, L.; Han, H.-H.; Bull, S.D.; He, X.-P.; James, T.D.; Sessler, J.L.; Tang, B.Z.; Tian, H.; Yoon, J. Excited-state intramolecular proton-transfer (ESIPT) based fluorescence sensors and imaging agents. *Chem. Soc. Rev.* **2018**, *47*, 8842–8880. [CrossRef]
5. Aiello, D.; Malfatti, L.; Kidchob, T.; Aiello, R.; Testa, F.; Aiello, I.; Ghedini, M.; La Deda, M.; Martino, T.; Casula, M.; et al. Blue-emitting mesoporous films prepared via incorporation of luminescent Schiff base zinc(II) complex. *J. Sol-Gel Sci. Technol.* **2008**, *47*, 283–289. [CrossRef]
6. Raditoiu, A.; Radițoiu, V.; Culita, D.C.; Baran, A.; Anghel, D.-F.; Spataru, C.I.; Amariutei, V.; Nicolae, C.A.; Wagner, L.E. Photophysical properties of some fluorescent materials containing 3-methoxy-7H-benzo[de]anthracen-7-one embedded in sol-gel silica hybrids. *Opt. Mater.* **2015**, *45*, 55–63. [CrossRef]
7. Deshpande, A.V.; Jathar, L.V.; Rane, J.R. Effect of method of preparation and drying time on photophysical properties of coumarin 1 laser dye embedded in HCl catalysed sol-gel glasses. *J. Non-Cryst. Solids* **2010**, *356*, 1–7. [CrossRef]
8. Sokolov, I.; Volkov, D.O. Ultrabright fluorescent mesoporous silica particles. *J. Mater. Chem.* **2010**, *20*, 4247–4250. [CrossRef]
9. Rawat, M.S.M.; Mal, S.; Singh, P. Photochromism in anils—A review. *Open Chem. J.* **2015**, *2*, 7–19. [CrossRef]
10. Lin, H.; Chang, X.; Yan, D.; Fang, W.-H.; Cui, G. Tuning excited-state-intramolecular-proton-transfer (ESIPT) process and emission by cocrystal formation: A combined experimental and theoretical study. *Chem. Sci.* **2017**, *8*, 2086–2090. [CrossRef]
11. Chen, C.-C.; Dou, L.; Zhu, R.; Chung, C.-H.; Song, T.-B.; Zheng, Y.B.; Hawks, S.; Li, G.; Weiss, P.S.; Yang, Y. Visibly transparent polymer solar cells produced by solution processing. *ACS Nano* **2012**, *6*, 7185–7190. [CrossRef] [PubMed]
12. Poojary, S.; Sunil, D.; Kekuda, D.; Sreenivasa, S. Fluorescent aromatic symmetrical azines: Synthesis and appraisal of their photophysical and electrochemical properties. *Opt. Mater.* **2018**, *85*, 1–7. [CrossRef]
13. Tang, W.; Xiang, Y.; Tong, A. salicylaldehyde azines as fluorophores of aggregation-induced emission enhancement characteristics. *J. Org. Chem.* **2009**, *74*, 2163–2166. [CrossRef]
14. Purcar, V.; Rădiţoiu, V.; Dumitru, A.; Nicolae, C.-A.; Frone, A.N.; Anastasescu, M.; Rădiţoiu, A.; Raduly, M.F.; Gabor, R.A.; Căprărescu, S. Antireflective coating based on TiO_2 nanoparticles modified with coupling agents via acid-catalyzed sol–gel method. *Appl. Surf. Sci.* **2019**, *487*, 819–824. [CrossRef]

15. Ziółek, M.; Filipczak, K.; Maciejewski, A. Spectroscopic and photophysical properties of salicylaldehyde azine (SAA) as a photochromic Schiff base suitable for heterogeneous studies. *Chem. Phys. Lett.* **2008**, *464*, 181–186. [CrossRef]
16. Rodríguez-Córdoba, W.; Zugazagoitia, J.S.; Collado-Fregoso, E.; Peón, J. Excited state intramolecular proton transfer in schiff bases. decay of the locally excited enol state observed by femtosecond resolved fluorescence. *J. Phys. Chem. A* **2007**, *111*, 6241–6247. [CrossRef]
17. Plotner, J.; Dreuw, A. Solid state fluorescence of pigment yellow 101 and derivatives: A conserved property of the individual molecules. *Phys. Chem. Chem. Phys.* **2006**, *8*, 1197–1204. [CrossRef]
18. Massue, J.; Felouat, A.; Vérité, P.M.; Jacquemin, D.; Cyprych, K.; Durko, M.; Sznitko, L.; Mysliwiec, J.; Ulrich, G. An extended excited-state intramolecular proton transfer (ESIPT) emitter for random lasing applications. *Phys. Chem. Chem. Phys.* **2018**, *20*, 19958–19963. [CrossRef]
19. Zhang, Z.; Gorman, B.P.; Dong, H.; Orozco-Teran, R.A.; Mueller, D.W.; Reidy, R.F. Investigation of polymerization and cyclization of dimethyldiethoxysilane. *J. Sol-Gel Sci. Technol.* **2003**, *28*, 159–165. [CrossRef]
20. Nocun, M.; Cholewa-Kowalska, K.; Łączka, M. Structure of hybrids based on TEOS-cyclic forms of siloxane system. *J. Mol. Struct.* **2009**, *938*, 24–28. [CrossRef]
21. Mah, S.K.; Chung, I.J. Effects of dimethyldiethoxysilane addition on tetraethylorthosilicate sol-gel process. *J. Non-Cryst. Solids* **1995**, *183*, 252–259. [CrossRef]
22. Wang, F.; Liu, J.; Luo, Z.; Zhang, Q.; Wang, P.; Liang, X.; Li, C.; Chen, J. Effects of dimethyldiethoxysilane addition on the sol–gel process of tetraethylorthosilicate. *J. Non-Cryst. Solids* **2007**, *353*, 321–326. [CrossRef]
23. Iacono, S.T.; Budy, S.M.; Mabry, J.M.; Smith, D.W. Synthesis, characterization, and surface morphology of pendant polyhedral oligomeric silsesquioxane perfluorocyclobutyl aryl ether copolymers. *Macomolecules* **2007**, *40*, 9517–9522. [CrossRef]
24. Guo, L.; Hyeon-Lee, J.; Beaucage, G. Structural analysis of poly(dimethylsiloxane) modified silica xerogels. *J. Non-Cryst. Solids* **1999**, *243*, 61–69. [CrossRef]
25. Tamayo, A.; Rubio, J. Structure modification by solvent addition into TEOS/PDMS hybrid materials. *J. Non-Cryst. Solids* **2010**, *356*, 1742–1748. [CrossRef]
26. Zheng, C.; Lin, A.; Zhen, X.; Feng, M.; Huang, J.; Zhan, H. Structural and textural evolution of dimethyl-modified silica xerogels. *Mater. Lett.* **2007**, *61*, 2927–2930. [CrossRef]
27. Xu, J.; Liu, Y.; Du, W.; Lei, W.; Si, X.; Zhou, T.; Lin, J.; Peng, L. Superhydrophobic silica antireflective coatings with high transmittance via one-step sol–gel process. *Thin Solid Films* **2017**, *631*, 193–199. [CrossRef]
28. Dreuw, A.; Plötner, J.; Lorenz, L.; Wachtveitl, J.; Djanhan, J.E.; Brüning, J.; Metz, T.; Bolte, M.; Schmidt, M.U. Molecular mechanism of the solid-state fluorescence behavior of the organic pigment yellow 101 and its derivatives. *Angew. Chem. Int. Ed.* **2005**, *44*, 7783–7786. [CrossRef]